

NASA-TM-112910

## Calculations of supersonic and hypersonic flows using compressible wall functions

P. G. Huang<sup>a</sup> and T. J. Coakley<sup>b</sup>

<sup>a</sup>Eloret Institute, Palo Alto, CA.

<sup>b</sup>NASA Ames Research Center, Moffett Field, CA.

### Abstract

The present paper presents a numerical procedure to calculate supersonic and hypersonic flows using the compressible law of the wall. The turbulence models under consideration include the Launder-Reece-Rodi-Gibson Reynolds-stress model and the  $k - \epsilon$  model. The models coupled with the proposed wall function technique have been tested in both separated and unseparated flows. The flows include (1) an insulated flat plate flow over a range of Mach numbers, (2) a Mach 5 flat plate flow with cold wall conditions, (3) a two dimensional supersonic compression corner flow, (4) a hypersonic flow over an axisymmetric flare and (5) a hypersonic flow over a 2-D compression corner. Results indicate that the wall function technique gives improved predictions of skin friction and heat transfer in separated flows compared with models using wall dampers. Predictions of the extent of separation are not improved over the wall damper models except with the Reynolds-stress model for the supersonic compression corner flow case.

### 1 Introduction

Historically, turbulence models are developed from some high Reynolds number closure. To apply the models in near-wall regions, two practices have been adapted to account for the low-Reynolds number effects; one by introducing additional viscosity dependent terms, and the other by applying the wall functions such as "the law of the wall" to bridge over the region very close to the wall.

The low-Reynolds-number models allow the complete set of governing equations to be integrated directly onto the solid-wall surface. This arrangement, although requiring more computer storage and time, allows the influence of force field (such as pressure gradients) and the variation in physical properties to be fed directly into the governing equations. However, an accurate model description of the near-wall behavior is not yet possible for complex flows for there is very little information available about the magnitude of individual terms in the energy and stress budget in the low-Reynolds number region.

Although recent direct numerical simulation data are available to guide the development of low-Reynolds number terms, they are limited only to simple attached flow cases. As a result, models developed under the attached-flow conditions remain to be thoroughly tested in regions where the flow is separated. Limited experience so far has shown that the existing uncorrected low-Reynolds-number turbulence models fail badly in predicting heat transfer with flow separation and this feature is observed in both incompressible [Yap and Launder, 1988] and compressible calculations [Coakley and Huang, 1992]. In addition, it has been found that none of the uncorrected low-Reynolds-number models successfully predicts the extent of the flow separation for the separated flows [Coakley and Huang, 1992]. Although model modifications have been found to improve predictions of some of these flows, the situation is not entirely satisfactory because the somewhat arbitrary nature of the modifications and their lack of generality.

Wall function techniques have been very popular in the past because on the one hand they contain no stiff low-Reynolds number terms and on the other hand they require less computer storage and time. Strictly speaking, the law of the wall can only be applied in attached flows with no pressure gradient and mass transfer, but it has been extrapolated to a variety of situations, including flow separation, with some surprisingly successful outcomes [Viegas and Rubesin, 1985]. It may be fair to say that unless a more definite low-Reynolds-number model has emerged to predict flow separation, the wall function techniques will still receive attention in predicting complex turbulent flows.

The purpose of this paper is to examine and compare the performance of models using wall functions with those using wall dampers for a set of simple and complex flows.

## 2 The compressible law of the wall

In this paper, we have restricted the discussion only to the conventional "single-layer" wall functions, i.e. the effects of the viscous sublayer is neglected. For a more complicated "two-layer" treatment, the reader should refer to Viegas and Rubesin [1985].

In compressible flow the usual "law of the wall" can be written exactly as in the constant-property case with the velocity defined by the Van Driest transformation,

$$U_c^+ = \frac{U_c}{U_\tau} = \frac{1}{\kappa} \ln y^+ + C \quad (1)$$

where  $U_\tau = \sqrt{\tau_w/\rho_w}$ ;  $y^+ = U_\tau y / \nu_w$ ;  $\kappa \approx 0.41$  is the von Kármán constant;  $C$  is chosen to be the same as its incompressible flow counterpart, 5.2, and this choice appears to be supported by the experimental data assembled by Fernholz and Finley [1980]; and finally  $U_c$  is the Van Driest transformed velocity defined by [Van Driest, 1951; Bradshaw, 1977 and Viegas and Rubesin, 1985]:

$$U_c = \sqrt{B} \left[ \sin^{-1}\left(\frac{A+U}{D}\right) - \sin^{-1}\left(\frac{A}{D}\right) \right] \quad (2)$$

where

$$\begin{aligned} A &= q_w / \tau_w \\ B &= 2 c_p T_w / Pr_t \\ D &= \sqrt{A^2 + B} \end{aligned}$$

In the derivation of these equations it has been assumed  $\tau = \tau_w$ , which implies zero-pressure gradient.

Near a solid surface, the convection can be neglected in comparison with viscous terms, and the energy equation can be integrated to give an expression for the total heat flux as;

$$q = q_w + U \tau \quad (3)$$

Equations (1) and (3) are used to bridge over the first grid point located inside the inner layer and the solid wall. The turbulence kinetic energy and its dissipation rate at the inner layer are fixed according to;

$$k = (\tau_w/\rho)/0.3 \quad (4)$$

$$\epsilon = \frac{(\tau_w/\rho)^{3/2}}{\kappa y} \quad (5)$$

It should be noted that  $\rho$  in (4) and (5) is the local value, instead of the wall value as in incompressible flows.

For Reynolds stress models, stresses are fixed in the inner layer with respect to the value of  $k$ . The ratios of the stresses to turbulence kinetic energy vary according to the model used. For the Launder-Reece-Rodi-Gibson model [Gibson and Launder, 1978], the stresses for the wall-oriented Cartesian frame of reference, denoted by “ $\wedge$ ”, are given according to [Lien and Leschziner, 1991];

$$\widehat{\overline{u^2}} = 1.0984k \quad (6)$$

$$\widehat{\overline{v^2}} = 0.2476k \quad (7)$$

$$\widehat{\overline{w^2}} = 0.654k \quad (8)$$

$$\widehat{\overline{uv}} = -\text{sign}(\hat{U})0.255k \quad (9)$$

### 3 Numerical aspects

The numerical procedure used here is based on an implicit line-by-line Gauss-Seidel algorithm using Roe's approximate Riemann solver coupled with Roe's "SUPERBEE" TVD numerical scheme [Huang and Coakley, 1992]. The grids adjacent to the wall are adapted with time-steps to enable the first  $y^+$  to be between 20 and 40. The space between the second grid and the third grid points is adjusted so as to satisfy  $\Delta y^+$  to be approximately equal to 1 and thereafter the grid is expanded in the  $y$ -direction with a given expansion ratio, which is determined based on the height and the total grid points prescribed. In general, at least 50 points inside the boundary layer are provided in the calculations.

The steps in implementing the law of the wall for compressible flows are outlined below. In the equations that follow,  $U_1$  is the velocity component parallel to the wall at the first mesh point above the wall;  $T_1$  is the corresponding temperature, and  $y_1$  is the normal distance from the wall.

1. Assuming  $y_1^+$  estimated initially or given from the previous time step, calculate  $U_{c,1}^+$  from equation (1).

2. Assuming  $q_w/\tau_w$  and  $T_w$  given initially or given from the previous time step, calculate  $U_{c,1}$  from equation (2).
3. Equation (1) is written in terms of a formula for the wall shear stress,  $\tau_w$ ;

$$\begin{aligned}\tau = \tau_w &= \rho_w U_\tau \frac{U_{c,1}}{U_{c,1}^+} \\ &= y_1^+ \mu_w \frac{U_{c,1}}{U_1} \frac{1}{U_{c,1}^+} \frac{U_1}{y_1}\end{aligned}\quad (10)$$

Here, one can define an effective turbulent viscosity connecting the wall and the first grid point,  $\mu_t = y_1^+ \mu_w U_{c,1}/(U_1 U_{c,1}^+)$ .

4. Substituting equation (10) into equation (3) and assuming a constant Prandtl number,  $Pr_t$ , the heat flux at the wall can be obtained;

$$q_w = -\frac{\mu_t c_p}{Pr_t} \frac{T_1 - T_w}{y_1} - \mu_t \frac{U_1^2}{2y_1} \quad (11)$$

which enables an effective turbulent conductivity,  $\mu_t c_p / Pr_t$ , to be used between the wall and the first grid point.

5. Solve for  $U_1$  and  $T_1$  from the Navier-Stokes equations.
6. Update  $\tau_w$  and  $q_w$  (or  $T_w$ ) from equations (10) and (11), respectively.
7. Redefine  $y_1^+$ .

Finally, all turbulence quantities are fixed at the first grid point according to equations (4) to (9). This treatment effectively moves the boundary conditions of the turbulence transport equations from the wall to the first grid point.

## 4 Results

Based on a comparison study of Hopkins and Inouye [1971], the Van Driest II theory was established as the most accurate procedure to extend the incompressible correlation to compressible flows. Figure 1 thus compares the skin friction predictions of flat plate boundary layer flows, with reference to the Van Driest II theory. The experimental data used by Hopkins and Inouye are also depicted in the figures.

Figure 1(a) shows the skin friction comparison of a flow over an adiabatic wall for Mach number ranging from 0.1 to 10. The comparison is made with the Van Driest II theory at  $Re_\theta = 10,000$ . It can be seen that results obtained from both the  $k - \epsilon$  and the Reynolds stress models using the proposed wall function technique agree very well with the theory, considering the fact that the experimental data spread  $\pm 10\%$  about the theory. For the high-Mach-number-flow cases, it can be seen that the present predictions give rise to skin friction values higher than those of the Van Driest II theory. No data is available to confirm this observation, however.

Figure 1(b) shows the comparison of the predictions with the Van Driest II theory at  $Re_\theta = 10,000$ , for the cooled-wall cases. The agreement with the theory is within the

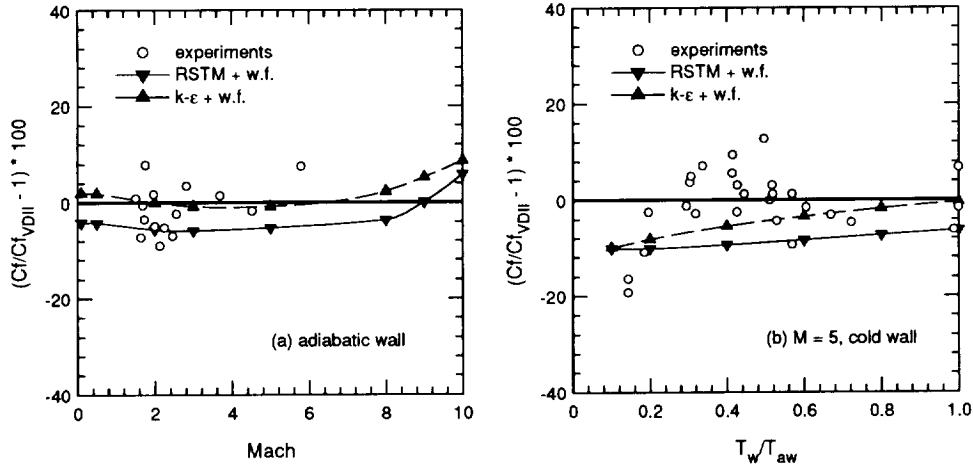


Figure 1: Skin-friction comparisons

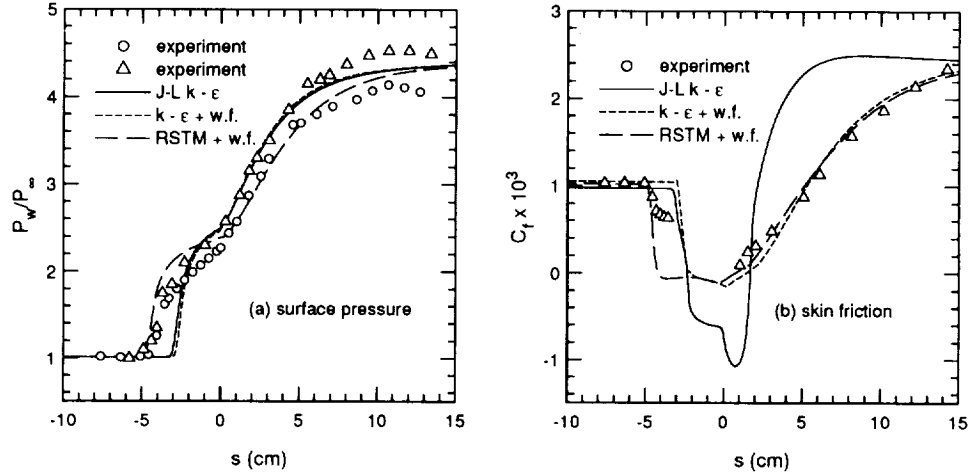
experimental data bound. However, it should be noted that the computed values have a tendency to fall away from the Van Driest II correlation in strong cooled wall conditions. This behavior appears to be supported by the limited experimental data comparison.

For both adiabatic and cooled wall, the  $k - \epsilon$  model gives a somewhat better solution than the Reynolds-stress model, but this is mainly due to the fact that the Reynolds-stress model predicts a lower value of skin friction at  $M = 0$ . The general trends of the predictive behavior of the two models, subject to the Mach number and the wall cooling effects, are similar.

The next three cases are calculations of the shock wave boundary layer interaction flows. The first is a supersonic flow over an almost adiabatic compression corner [Settles et. al., 1980], the second is a hypersonic flow over a cooled axisymmetric flare [Kussoy and Horstman, 1989] and the third is a hypersonic flow over a cooled 2-D compression corner [Coleman, 1972]. The choice of these cases is guided by the recommended database evaluated by Settles and Dodson [1991].

Figure 2 show the results of a  $24^\circ$  compression corner flow at  $M = 2.84$  [Settles et. al., 1980]. The Reynolds stress model predicts an earlier separation (i.e. pressure rise) than the  $k - \epsilon$  model and agrees better with the experimental data. The earlier separation offered by the Reynolds stress model is consistent with incompressible calculation experiences. After the re-attachment, both models predict a similar skin-friction recovery behavior, which agrees very well with the experimental data. For the purpose of comparison, the result obtained by the Jones-Launder low-Reynolds-number  $k - \epsilon$  model [1972] using the modified Sharma-Launder constants [1974] is also presented in the figure. It can be seen that this model not only fails to predict flow separation but also gives rise to too fast a skin-friction recovery downstream of flow re-attachment.

In figure 3, the surface pressure and heat transfer predictions of the hypersonic cylinder-

Figure 2: Supersonic 2-D compression corner flow,  $24^\circ$  and  $M = 2.84$ 

flare flow are shown. The results are presented for the flare angle of  $35^\circ$  and a freestream Mach number of 7.05. It can be seen from the comparison of the surface pressure, shown in figure 3(a), the wall function technique, irrespective of the models used, predicts very little separation and hence the pressure peak near flow re-attachment is not predicted correctly. Similarly, the low-Reynolds-number  $k - \epsilon$  model produces a too small separation similar to that obtained by using the wall function technique. It should be noted that, for some unknown reasons, the Reynolds stress model *did not* increase the size of the separation bubble, as observed in subsonic and supersonic calculations [Leschziner, 1986; Lien and Leschziner, 1991].

One of the major improvements of the wall function technique over the low-Reynolds number models is depicted in the prediction of the surface heat transfer, figure 3(b). The low-Reynolds number  $k - \epsilon$  models over-predict the heat transfer near re-attachment by a factor of three times the experimental value. Although not shown here, it should be noted that this feature is observed in *all* the well-known low-Reynolds number two-equation models [Coakley and Huang, 1992]. In addition, this inaccurate behavior was also reported by Yap and Launder [1988] who calculated the heat transfer of an *incompressible* back-step flow. Coakley and Huang [1992] have demonstrated that by limiting the length scale of the near wall region with respect to the von Kármán length scale, the heat transfer near the re-attachment regions can be reduced to the experimental level. The better agreement of the heat transfer predictions offered by the models using the wall function technique supports this observation, because the wall function approach implicitly contains the von Kármán length scale concept.

The surface-pressure and heat-transfer predictions of the hypersonic 2-D compression corner are shown in figure 4. The results are presented for the flare angle of  $34^\circ$  and a freestream Mach number of 9.22. The predicted behavior is very similar to that of the

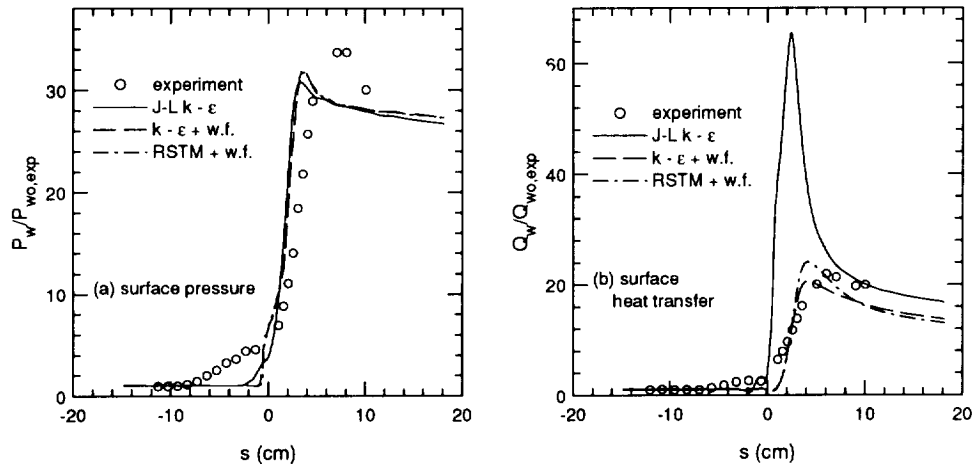


Figure 3: Hypersonic cylinder-flare,  $35^\circ$  and  $M = 7.05$

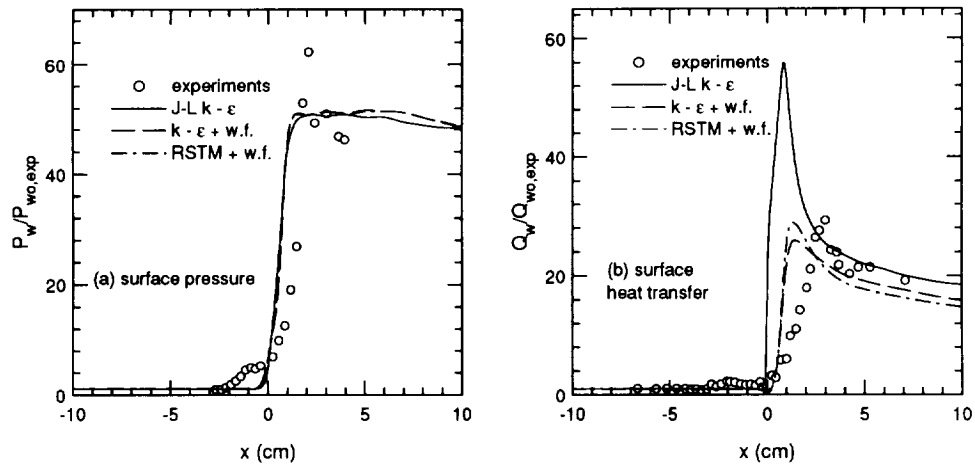


Figure 4: Hypersonic 2-D compression corner,  $34^\circ$  and  $M = 9.22$

previous case. Both the  $k - \epsilon$  and the Reynolds-stress models fail to predict the size of the separation and hence the peak of the pressure rise near flow re-attachment, but were able to predict the right level of heat transfer near the flow re-attachment regions. In contrast, the low-Reynolds number model not only failed to predict the size of flow separation but also over-predicted the heat transfer rate by approximately two times the experimental values near the flow re-attachment regions.

## 5 Concluding remarks

The Van Driest transformation is used to extended the incompressible wall functions to compressible calculations. The numerical methods required to implement the compressible wall functions for both supersonic and hypersonic calculations are reported.

For a flat plate zero-pressure-gradient boundary layer flow, both the Reynolds stress and the  $k - \epsilon$  models produce satisfactory skin friction predictions compared with the experimental data.

In contrast to the low-Reynolds-number  $k - \epsilon$  model, both the Reynolds stress and the  $k - \epsilon$  models predict excellent skin-friction recovery behavior for the supersonic compression corner case. Similar to the incompressible calculation experience, the separation bubble produced by the Reynolds stress model better agrees with the experimental data while the  $k - \epsilon$  model under-predicts the size of separation. Unfortunately, for hypersonic flow calculations, both the  $k - \epsilon$  and the Reynolds stress models fail to predict the size of the flow separation and their results are very similar. The heat transfer rate near the flow re-attachment regions is better represented by the model predictions using the wall function technique, because the low-Reynolds-number  $k - \epsilon$  model produces peak heat transfer rates 2 to 3 times higher than the experimental values.

## References

- [1] Bradshaw, P. 1977. "Compressible turbulent shear layers," *Annual Reviews of Fluid Mechanics*, 9, pp 33-54.
- [2] Coakley, T. J. & Huang, P. G. 1992. "Turbulence modeling for high speed flows," AIAA paper 92-0436, Reno, Nevada.
- [3] Fernholz, H. H. & Finley, P. J. 1980. "A critical commentary on mean flow data for two-dimensional compressible turbulent boundary layers," AGARD-AG-253.
- [4] Gibson, M. M. & Launder, B. E. 1978. "Ground effects on pressure fluctuations in the atmospheric boundary layer," *J. Fluid Mech.*, 85, p 491.
- [5] Hopkins, E. J. & Inouye, M. 1971. "An evaluation of theories for predicting turbulent skin friction and heat transfer on flat plates at supersonic and hypersonic Mach number," *AIAA J.*, 9, 6, pp. 993-1003.
- [6] Huang, P. G. & Coakley, T. J. 1992. "An implicit Navier-Stokes code for turbulent flow modeling," AIAA paper 92-0547, Reno, Nevada.

- [7] Jones, W. P. & Launder, B. E. 1972. "The prediction of laminarization with a two equation model of turbulence," *Int. J. of Heat and Mass Transfer*, 15, pp. 301-304.
- [8] Kussoy, M. I. & Horstman, C. C. 1989. "Documentation of two- and three-dimensional hypersonic shock wave turbulent boundary layer interaction flows," *NASA TM 101075*.
- [9] Launder, B. E. & Sharma, B. I. 1974. "Application of the energy-dissipation model of turbulence to the calculation of flow near a spinning disk," *Letters in Heat and Mass Transfer*, 1, pp. 131-138.
- [10] Lien, F. S. & Leschziner, M. A. 1991. "Second-moment modelling of recirculating flow with a non-orthogonal collocated finite-volume algorithm," *Eighth Symposium on Turbulent Shear Flows*, Munich, Germany.
- [11] Leschziner, M. A. 1986. "Finite-volume computation of recirculating flow with Reynolds-stress turbulence closures," *3rd Int. Conf. on Numerical Methods for Non-linear Problems*, Dubrovnik, Croatia.
- [12] Settles, G. S. & Dodson, L. J. 1991. "Hypersonic shock/boundary-layer interaction database," *NASA Contractor Report 177577*.
- [13] Settles, G. S., Gilbert, R. B. & Bogdonoff, S. M. 1980. "Data compilation for shock wave/turbulent boundary layer interaction experiments on two-dimensional compression corners," *Princeton University Report 1489-MAE*, Princeton University.
- [14] Van Driest, E. R. 1951. "Turbulent boundary layer in compression fluids," *J. Aeronaut. Sci.*, 18, pp 145-160.
- [15] Viegas, J. R. & Rubesin, M. W. 1985. "On the use of wall-functions as boundary conditions for two-dimensional separated compressible flows," *AIAA paper 85-0180*, Reno, Nevada.
- [16] Yap, C. & Launder B. E. 1988. "Prediction of corrective heat transfer in impinging and separating flow," *3rd Biennial Colloquium on CFD*, UMIST.





